Smectite flocculation structure modified by Al_{13} macromolecules; as revealed by the Transmission X-ray Microscopy (TXM)

Marek S. Żbik, Wayde N. Martens, Ray L. Frost, •
Inorganic Materials Research Program, School of Physical and Chemical Sciences, Queensland University of Technology 2 George Street, GPO Box 2434, Brisbane Qld 4001 Australia.

Yen-Fang Song, Yi-Ming Chen, Jian-Hua Chen
National Synchrotron Radiation Research Center, 101 Hsin-Ann Road, Hsinchu Science Park, Hsinchu 30076, Taiwan, R.O.C.

Corresponding Author: Ray L. Frost

E: r.frost@qut.edu.au

P: +61 7 3138 2407

F: +61 7 3138 1804

• Author to whom correspondence should be addressed (r.frost@qut.edu.au)

Smectite flocculation structure modified by Al_{13} macromolecules; as revealed by the Transmission X-ray Microscopy (TXM)

Marek S. Żbik, Wayde N. Martens, Ray L. Frost, •
Inorganic Materials Research Program, School of Physical and Chemical Sciences, Queensland University of Technology 2 George Street, GPO Box 2434, Brisbane Qld 4001 Australia.

Yen-Fang Song, Yi-Ming Chen, Jian-Hua Chen
National Synchrotron Radiation Research Center, 101 Hsin-Ann Road, Hsinchu Science Park, Hsinchu 30076, Taiwan, R.O.C.

Abstract

The aggregate structure which occurs in aqueous smectitic suspensions is responsible for poor water clarification, difficulties in sludge dewatering and the unusual rheological behaviour of smectite rich soils. These macroscopic properties are dictated by the 3-D structural arrangement of smectite finest fraction within flocculated aggregates. Here, we report results from a relatively new technique, Transmission X-ray Microscopy (TXM), which makes it possible to investigate the internal structure and 3-D tomographic reconstruction of the smectite clay aggregates modified by Al_{13} keggin macro-molecule $[Al_{13}(O)_4(OH)_{24}(H_2O)_{12}]^{7+}$. Three different treatment methods were shown resulted in three different micro-structural environments of the resulting flocculation.

Keywords: Transmission X-ray Microscopy, Keggin structure, smectite, flocculation

1. Introduction

Smectites are clay minerals commonly found as components of soils from temperate climates. Smectites are formed as result of the weathering of volcanic glass which is abundant in ash-beds and basic rocks like basalts. Smectites are useful for dam bed impregnation, to improve water retention properties and as drilling mud, to seal the cut, thus

• Author to whom correspondence should be addressed (r.frost@qut.edu.au)

preventing fluid loss. They are also popular stabilising additives in engine oils, cosmetics, pharmaceutical and chemical industries.

Smectite's unusual macroscopic properties are dominated by its structural arrangement and the morphology of its finest fraction. These clays are extremely dispersed and exhibit very high surface area of several hundred square meters per gram. High smectite dispersion in water makes this group of minerals very attractive as the crude base to all game of nano-materials manufacturing for various applications. These applications use the materials high porosity, high sorption capacity and high surface area for catalytic purposes. Intercalated and pillared clays have attracted increasing attention, particularly from industry since the 1970s, because of their microporous nature and catalytic potential. All clay modifications like cation exchange, pH variation, intercalation and other techniques aims to change the structural matrix of resultant material and this determining the resulting material properties.

Comment [m1]: Does not make sense

The first attempt to describe the microstructure of clays was made by Terzaghi [1], who proposed the honeycomb model as the structural basis of water saturated clays. Subsequent investigations based on the development of new techniques in electron-microscopes [2] confirm the existence of the "card house" structure Rosenquist [3], Bowles [4]. Pusch [5] confirmed the presence of the honeycomb microstructure in wet clay sediments. Cryo-SEM investigation in O'Brien [6] published a large amount of microstructural data. Given the size of the clay constituents, SEM was found to be the tool of choice used by scientists studying the microstructure of smectitic clays [7]. Most recently Synchrotron based Transmission X-Ray Microscopy (TXM) allowing 3-D examination of examined structure in stereo pares as well as in computer calculated 3-D reconstruction [8, 9].

From numbers of smectite modification agents we chose intercalation and cation exchange by Al_{13} Keggin-like macromolecule in present investigation. This is because of high positive charge of this molecule which may have significant impact on resulting smectite aggregate structure in aqueous suspensions. Further to this this research has profound implications for the water purification industry where alum or aluminium chlorohydarte is used. In the present article we present the microstructure of resulting aggregates as observed by the TXM technique.

Sample preparation methods available for cryo-investigations in electron microscopy techniques, like partial freeze drying, critical point-drying and cryo-fixation, have been found

to introduce many artefacts especially when applied to the study of clay suspension or gel structure [10]. These artifacts result as a consequence of the low thermal conductivity of water and ice, which only allows a slow rate of heat withdrawal from the specimen. Thus, TXM method which allowed observation of clay particles in water without any pre-preparation is free of above mentioned artefacts and was chosen in conducting present investigations.

2. Experimental Section

During the last decade the TXM technique has been implemented to the study of clay aggregate structure in aqueous environment science, nano-tomography. This method is based on the transmission X-ray microscopy, which works with a synchrotron photon source at the BL01B1 endstation of the National Synchrotron Radiation Research Center (NSRRC) [11]. This new technique [12] has recently been established to investigate clay suspension in an aqueous environment, without sample preparation. The big advantage of TXM tomography, is that without sample pre-treatment it is possible, for the first time, to observe clay microstructure in an aqueous environment, artefact free.

The smectite used in this study was a well known Na-montmorillonite from Wyoming (U.S.A.), obtained from Clay Science Society. The original clay sample (SWy-2) has been well described [13] and the two samples were prepared from this original clay. First, the colloidal fraction was separated by centrifugation and secondly, all cations in exchangeable positions were ion exchanged with Al_{13}^{7+} ions. Experiments were performed in distilled water.

The cluster cation $(Al_{13}O_4(OH)_{24}(H_2O)_{12})^{7+}$ has the Keggin structure with a tetrahedral Al atom in the centre of the cluster coordinated to 4 oxygen atoms [14]. This ion is generally called the Al_{13} ion. A Ga_{13} analogue is known [15] and also was used in our experiments to investigate whether Ga atoms have greater absorption and hence contrast than Al atoms.

Preparation of intercalated Swy-2 montmorillonite and solutions of aluminium and gallium 13 keggin ions where prepared by a method similar to Doung et al. [16]. Solutions of sodium hydroxide (0.10M), aluminium nitrate (0.05M) and gallium nitrate (0.05M) were prepared in filtered water (18.2MΩ). A peristaltic pump was used to add the hydroxide

117 solution (0.125% of the solution per minute) to a solution of the metal nitrate in a molar ratio
118 of 2:1 (hydroxide: metal). The resultant keggin ion solution was allowed to age over night
119 before use. To an aliquot of the keggin ion solution, the sodium exchanged Swy-2 was added
120 in an amount which ensured the keggin ion remained four times the CEC. The clay in keggin
121 ion solution was mixed overnight using a magnetic stirrer before collection, washing and
122 drying via vacuum filtration. The keggin ion exchanged SWy-2 was subjected to x-ray
123 diffraction to ensure complete exchange as shown in Fig. 1.
124

Comment [m2]: We should give this information

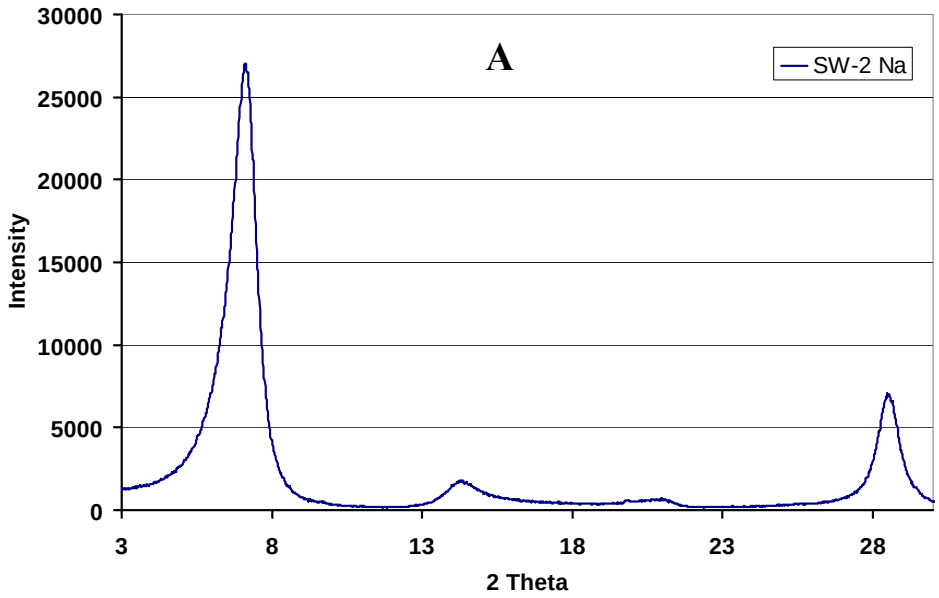

125

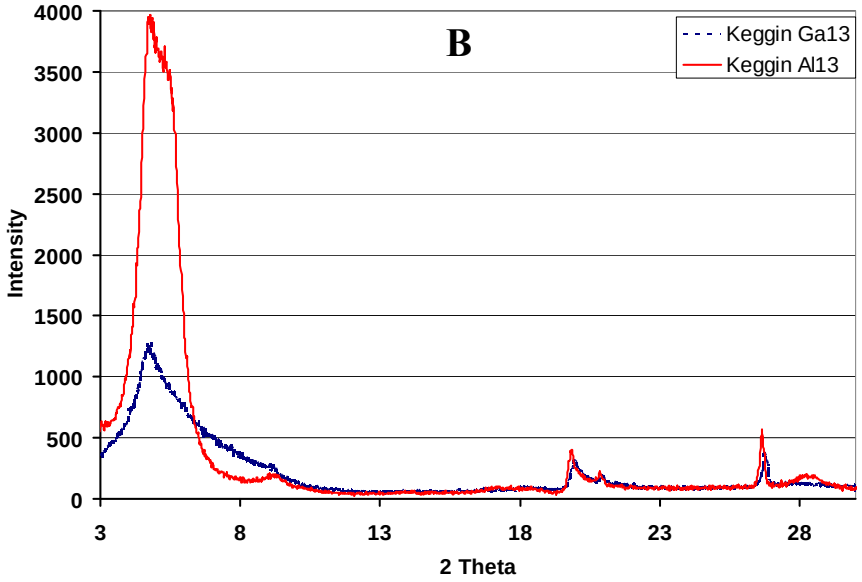

Fig. 1- XRD of the colloidal fraction of (A)- natural Na SW-2 show significant 001 peak in xxnm, (B)- after intercalation by Al13 and Ga 13 the mine 001 peak shifted towards larger separation distances.

Comment [m3]: Figure needs redoing please send the original files

A 10 % w/v suspension of the keggin exchanged Swy-2 was prepared from dried sample (Sample 0) by redispersing it in filtered water. In addition to this method, two other ways of smectite intercalation were performed to avoid the drying and redispersion step. One method (Sample 1) was prepared by addition of keggin diluted solution to smectite suspension which visibly resulted in gelation. A second method (Sample 2) based on addition of powdered smectite into diluted keggin solution which destabilised the smectite into flocculated aggregates. To all suspensions an aliquot (3 µl/ml of suspension) of 1mg/L gold nanoparticles (0.8-0.5 µm) was added.

Sample of one nano-liter of suspension was placed on the Capton tape within a silicon/silicon nitride and metal frame of sample holder about 3 cm in diameter. To prevent water evaporation during the time of experiment samples were covered by another layer of Capton tape. The prepared suspension was kept between two layers of Capton tape of thickness about 100 nm was mounted in sample stage within the beamline of X-rays in TXM and investigated.

Comment [m4]: This does not sound correct as I could see the thickness.

3. Results and discussion

Smectite represents a 2:1 type layer silicate with an expandable structure carrying a certain amount of excess negative layer charge comprising of sheets linked by weak van der Waals forces. The layered structure consists of an octahedral alumina sheet sandwiched between two tetrahedral silica sheets.

From microscopical observations [17], smectite consists of relatively large, flexible sheets with lateral dimension of ~800 -1000 nm and thickness of ~1-10 nm. The platelet assembly of the sheets are stacked on top of each other, in a parallel fashion called a tactoid (stacks of parallel clay platelets at – 10 Á separation). Due to bonding between individual sheets being very weak, the sheets easily slide along the top of each other and are quite flexible. Individual smectite sheets can be as thin as about 1 nm. Sodium smectite in a water suspension forms a gel where the tactoid sheets are highly flexible, individual particles and interact by a combination of edge attraction and basal plane repulsion. These properties build an expanded and extremely voluminous cellular network, composed of chain-like sheet assemblies similar to those described in the cryo-SEM and TXM micrograph [18]. In such an extended cellular network, flexible smectite sheets encapsulate water within cellular voids of dimensions up to 0.5-2 μm is known to span all volume of clay slurry, or produce separate aggregates. The AFM force measurements presented by authors show long range repulsion in range similar to observed cellular dimensions which were reduced in half in distances when Ca^{2+} cations were in exchangeable positions. This unusual long interaction was explained by some sort of steric interactions between smectite sheet tactoids.

In can be true as has been seen in the TEM micrographs in Fig. 2. In micrograph Fig. 2A, smectite plate with Na^{+} cations in exchangeable positions shows extended layer of loose "hairy" texture which may resemble the diffusion layer from double layer electrokinetic theory. This layer is more than 200 nm thick, but sample was dried to be investigated in SEM. This layer may be significantly larger within water environment and it may be responsible for described in [18] steric repulsion. In smectite with Ca^{2+} cations in exchangeable positions like shown in Fig. 1B such a layer is depressed to within 50 nm distance from platelet surface.

Comment [m5]: Figure 1A is XRD

Our examination of smectite behaviour when intercalated with Al_{13} keggin ions in comparison to previously described Na^+ and Ca forms was prime focus in present study.

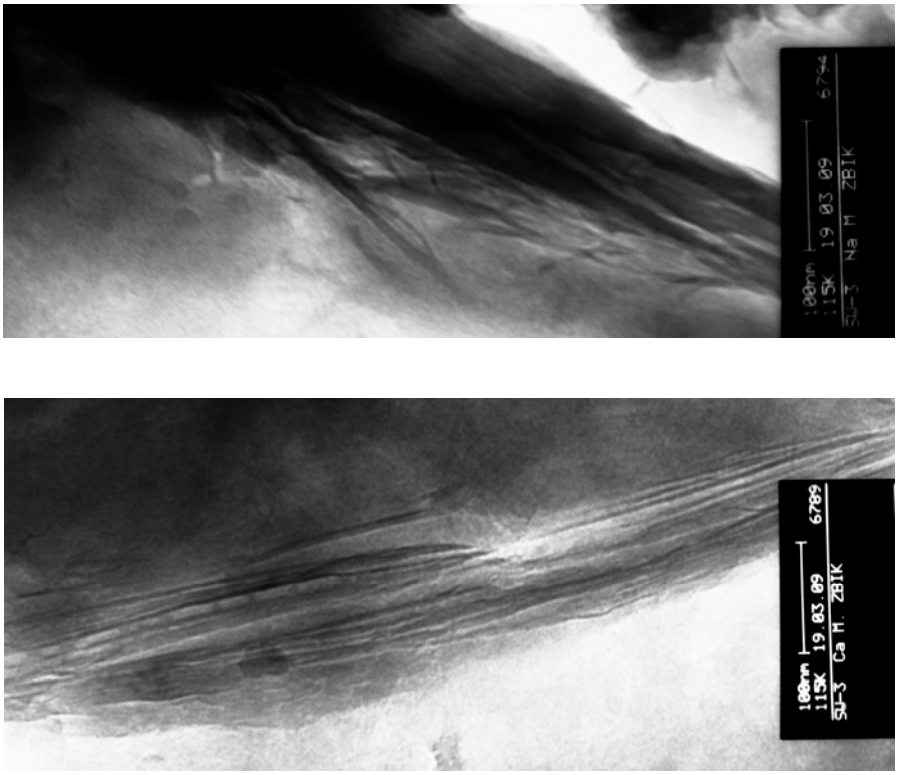

Fig. 2 TEM micrographs of (A)- Na^{+} and (B)- Ca^{2+} smectite flakes shown significant roughness at the platelet surface 200 nm extended in the Na^{+} and ~50 nm in Ca^{2+} exchangeable forms.

TEM micrographs taken from Ga/Al_{13} treated smectite, shown in Fig. 3 display compacted taktoid sheet with possible loosen fragments not extended beyond about 10 nm from platelet surface. This platelets looks much compacted than smectite sodium and calcium variations. This platelet looks more rigid and compact and separated individual smectite layer are very close together which may hardly allow water to penetrate interlayer area. In fact it was impossible to redisperse in water dried fragments of keggin modified smectite without grinding it.

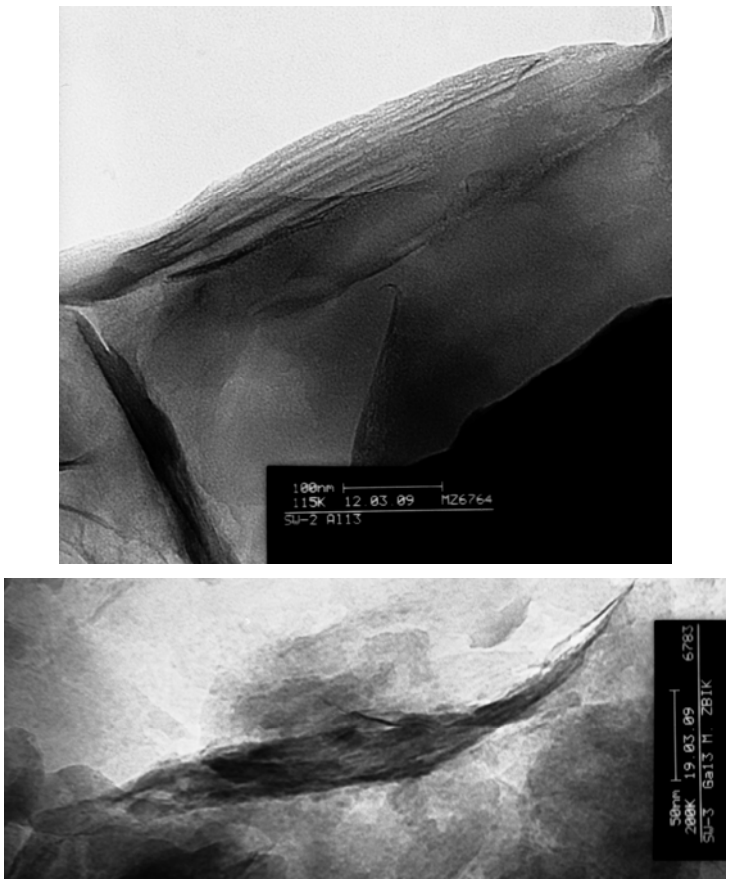

Fig. 3 TEM micrographs showing keggin treated smectite display compacted taktoid sheet with highly depressed surface loose material layer to maximum 10 nm.

In 10 wt% water suspension studied in TXM singular taktoids similar like shown in the TEM in Fig. 3 are connected in chain stairstep arrangements and produced irregular cellular, spongy network like shown in the TXM stereo-pare Fig. 4. Taktoids connecting each other by edges produce twisted chains which resemble closed loops. These loops of irregular shape are connected to neighbour similar structure and assembling spongy 3-D cellular network with irregular cells up to 0.5-1.5 μm in diameter.

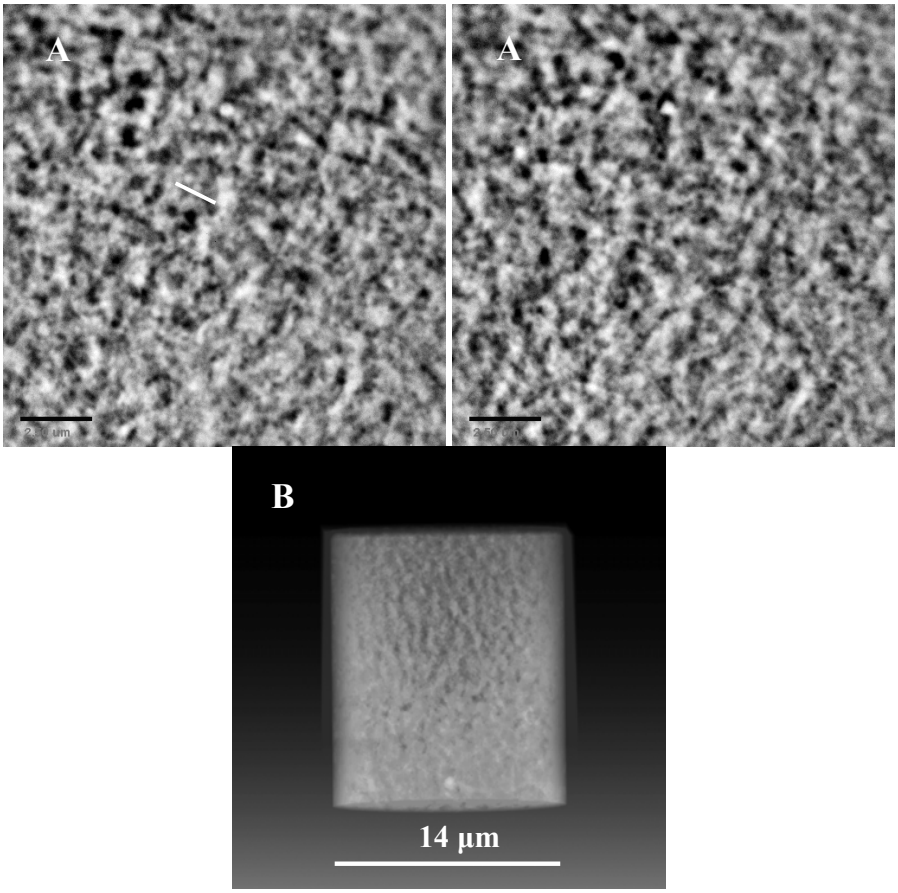

Fig. 4 TXM stereo-pare micrographs (A) shot with 1 degree difference in angle (Sample 0), reveals spongy irregular network of compact tactoids connecting with each other in chain stairstep aggregates assembling cells up to 1.5 µm in diameter (shown as a white bar in left micrograph). The 3-D computer reconstruction (B) shows large cellular pattern of microstructure with thick elongated walls composed of stairstep-like stacked smectite tactoids.

Cells look clear inside and whole structure appears to be stabilised by strength of the chain assembly and forces between contacting platelets. Elongated walls of cellular pattern consist with thick (up to 300 nm) aggregates of stairstep-like arranged tactoids can be observed in the 3-D computer reconstruction from tomographic investigation conducted using TXM (Fig. 4B).

Comment [m6]: Is it friction of attraction

Very different structure from described in Sample 0 was observed when keggin solution was added to 10 wt% smectite suspension (Sample 1). Suspension was instantly gelled in form of thick creamy substance. In TXM stereo-pare micrographs shown in Fig. 5 display individual tactoids connected in edge to face (EF) and face to face (FF) orientation living very porous honeycomb-like network of mostly regular voids up to 200 nm in diameter. Some numbers of taktoids resembled in FF orientations build small aggregates connected with similar aggregates by EF orientation.

This network of dense honeycomb-like particles form larger clusters 2-5 μm in diameter. These clusters contacting themself by few linking tactoids or display the fissure-like gaps up to 500 nm thick sporadically linked by singular tactoids.

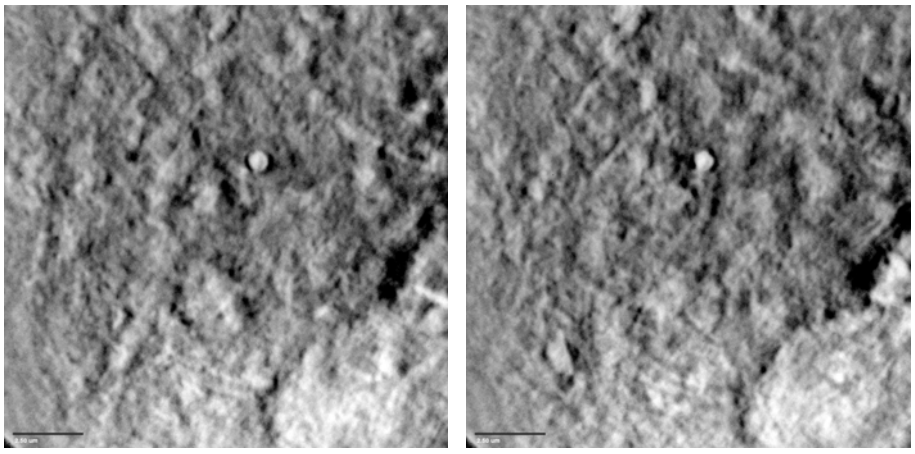

Fig. 5 TXM stereo-pare micrographs shot with 1 degree difference in angle in Sample 1 (gelled by addition of keggin to smectite suspension) reveal single tactoids connected in edge to face and face to face orientation living voids in between particles up to 200 nm in diameter. White spherical particle near the middle of micrograph is gold nano-particle introduced to sample for better alignment.

Similar cellular honeycomb-like network within porous cluster is recognisable in 3-D reconstruction shown in Fig. 6. Resolution in this computerised reconstruction seen in 2-D reproduction is much lower than in presented stereo-pares but this reconstruction is much better visible in computer 3-D model when rotated in different angles which gives much more information about character of networking.

Comment [m7]: Place the 3D thing in the supplementary material

From TXM 3-D examination we may conclude that inter-tactoid void system is free of particles within method resolution (60 nm).

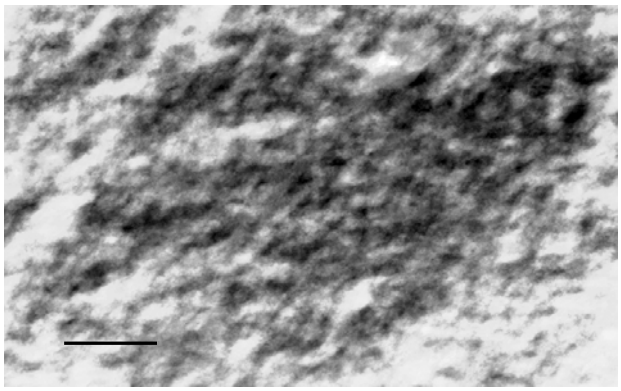

Fig. 6 Computer 3-D reconstruction of TXM tomography in Sample 1, shows cellular honeycomb like networking between smectite tactoids (scale bar 1 μm).

TXM investigation conducted on the flocculated Sample 2 revealed another type of micro-structure. Here, tactoids are stacked on top of each other in FF arrangement, form compact aggregates in shape of worms 0.5 to 3 μm long. These worms-like aggregates sometimes are linked and twisted with each other and difficult to follow up for longer distances. The stereo-pares in Fig. 7 this structure is visible, but partly masked by white colloidal material of uncertain origin covering these stacks. Fissure-like gaps between worm-like aggregates are only voids visible in this sample.

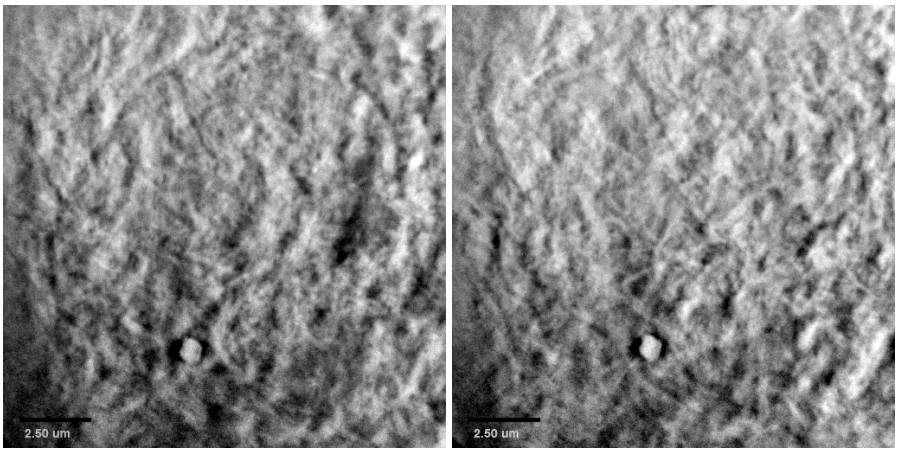

Fig. 7 TXM stereo-pare micrographs shot with 1 degree difference in angle in Sample 2 (flocked during addition of smectite to dilute keggin solution). Long worm-like stacked aggregates of smectite tactoids are covered by white colloidal blanket.

Similar FF stacked smectite tactoids visible in 3-D reconstruction shown in Fig. 8. Stacking not always going into single direction and in many places particles are shifting and starting "Y" shaping worm which may form separate aggregate after braking link. Aggregates, apart from occasional twisting and linking are clearly separated from each other and do not form spanning network like in two above described samples (Samples 0&1). These separations between aggregates give instability for this suspension and reasonable fast sedimentation of all mass of keggin treated dry smectite (Sample2).

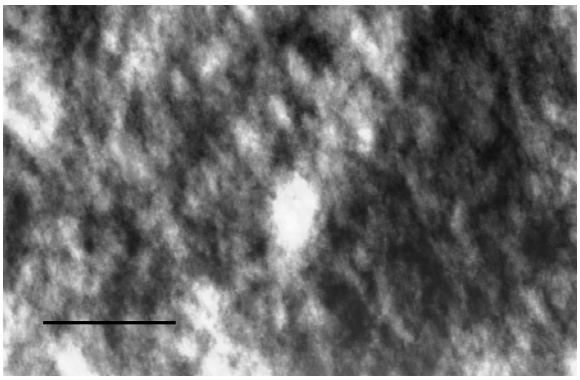

Fig. 8 Computer 3-D reconstruction of TXM tomography in Sample 2, shows stacked worm-like aggregates with voids in-between them (scale bar 2 μm).

After about 30 hours from collecting sample from containers and placing it into sample holders we noticed significant sample flocculation probably due to changing pore water pH or water evaporation. Capton foil may not be waterproof and in time some changes in water chemistry may occur. The occurrence of large even macroscopically visible flocks may results of these changes. As it is shown in the 3-D computer reconstruction of tomographic investigations in TXM, the large scale-like floccules are visible in Fig. 9. Floccules shown in Sample 1 (Fig. 9A) appear lighter, thinner and living shape of empty spherical voids in comparison with massive and compact floccules in Sample 2 with irregular inter-aggregate voids (Fig. 9B). All changes in the flock morphology may have to happen within suspension by particle orientation rearrangement and massive microstructure reformation.

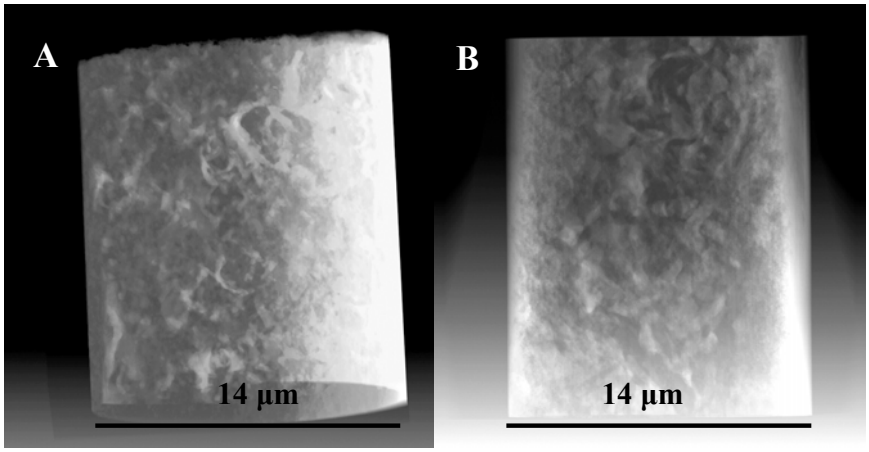

Fig. 9 The 3-D computer reconstruction of TXM tomography in Sample 1, (A) and Sample 2 (B). In this investigations both samples show significant degree of flocculation with fine cellular structure with large voids and thinner walls in Sample 1 and irregular inter-aggregate voids and thick dense aggregates in Sample 2.

4. Conclusions

Because TXM based on the synchrotron photon source is relatively new and is in rapid development, in this work we report the first attempt to study smectite gel structure in an aqueous environment. The images may be not giving very impressive micrographs as compared with other well established electron microscopy techniques, but enable us to observe clay aggregates within water, which has never been previously possible. A 3-D space reconstruction was obtained from 140 of 2-D images like shown in presented in paper stereo-pares, observed from angles +70 to -70 degrees. In this way gelled suspension is able to be observed from different angles. Such a reconstruction reveals, for the first time, number of variation of cellular micro-structural morphology of associated mineral sheets within water. Individual colloidal size particles are not well visible in this still picture however distinctive spongy and cellular structure is visible especially when carefully observing this reconstruction when rotating this image which cannot be demonstrated here in 2-D prints.

Cellular network composed by elongated aggregates of compact smectite modified flakes arranged in stair steps (FF) orientation of diameter in ranges 0.5 to 1 µm is visible in sample produced from intercalated dry smectite redispersed in water.

Much smaller voids of diameter ~200 nm were observed between mostly randomly oriented intercalated smectite flakes when gelled in effect of keggin addition to smectite suspension. These flakes randomly positioned in space are in EE and mostly EF orientation and build spanning network.

The keggin modified smectite by addition of dried smectite to dilute keggin solution display even another microstructural type where dense smectite flakes stacked in FF orientation build worm-like long aggregates. These aggregates are not bridged to other similar aggregates, fast settling and display narrow inter-aggregate voids in resulting sediment.

Described different microstructural types are probably reflects difference in the Gibbs energy position and DLVO theory. In case of smectite Sample 2 particles fall into the primary minimum where Van der Waals forces act between FF oriented smectite flakes and aggregates become approach irreversible flocculation. In case of Sample 1 particles contacting by edges (EE) and edge to face (EF) orientation fell into secondary minimum and weak flocculation resulted in severe gelation.

Comment [m9]: Can we measure the zeta potential and do the force measurements to confirm this?

Acknowledgements This work was supported by the Australian Synchrotron Research Program (ASRP).

Acknowledgements The financial and infra-structure support of the Queensland University of Technology Inorganic Materials Research Program of the School of Physical and Chemical Sciences is gratefully acknowledged. The Australian Research Council (ARC) is thanked for funding.

References:

[1] Terzaghi, K. Erdbaummechanik auf Bodenphysikalischer Grundlage. Franz Deuticke Press, Leipzig und Vienna 1925.

[2] Van Olphen, H. An Introduction to Clay Colloid Chemistry. Intersci. Publishers, N.Y. 1963

[3] Rosenquist, J.T. J. Soil Mech. And Found. Division, Proc. ASCE Sm 2, 85 (1959) 31-53

[4] Bowles, F.A. Science, 159 (1968) 1236-1237.

[5] Pusch, R. Clay Microstructure. National Swedish Building Research, Document D8, 1970

[6] O'Brien, N.R. Clays and Clay Minerals, 19 (1971) 353-359.

[7] Grabowska-Olszewska, B.; Osipov, V.; Sokolov, Vi. Atlas of the Microstructure of Clay Soils. PWN, Warszawa, 1984.

[8] Zbik, M. S., Frost, R. L., Song, Y-F. Journal of Colloid and Interface Science 319 (2008) 169-174.

[9] Zbik, M. S., Frost, R. L., Song, Y-F., Chen, Yi-M., Chen, J-H. Journal of Colloid and Interface Science 319 (2008) 457-461.

[10] M.S. Zbik, R.St.C. Smart, G.E. Morris, Journal of Colloid and Interface Science, 328 (2008) 73-80

[11] Attwood, D. Nature, 442 (2006) 642-643.

[12] Yin, G. C.; Tang, M. T.; Song, Y. F.; Chen, F. R.; Liang, K. S.; Duewer, F. W.; Yun, W.; Ko, D.H.; Shieh, H-P.D. Appl. Phys. Lett, 88 (2006) 241115-1241115-3.

[13] Van Olphen, H.; Fripiat J. J. Data handbook for clay materials and other non-metallic minerals. Oxford; New York. Pergamon Press. 1979, 183.

[14] Greenwood, Norman N.; Earnshaw, A. Chemistry of the Elements, 2nd Edition, Oxford: Butterworth-Heinemann. 1997.

[15] Bradley, S. M. Kydd, R. A. and Yamdagni. R. J. Chem. Soc., Dalton Trans., 1990, 413 – 417.

[16] Doung et al, Microporous and mesoporous materials, 82 (2005) 165.

[17] Morris G.E., Zbik, M.S. International Journal of Mineral Processing, 93 (2009) 20-25.

376 [18] Zbik, M.S. Martens, W., Frost, R. L., Song, Y-F., Chen, Yi-M., Chen, J-H. Langmuir, 24 (2008)
377 8954-8958.
378

List of Figures

Fig. 1- XRD of the colloidal fraction of (A)- natural Na SW-2 show significant 001 peak in xxnm, (B)- after intercalation by Al13 and Ga 13 the mine 001 peak shifted towards larger separation distances.

Comment [m10]: Figure needs redoing please send the original files

Fig. 2 TEM micrographs of (A)- Na^{+} and (B)- Ca^{2+} smectite flakes shown significant roughness at the platelet surface 200 nm extended in the Na^{+} and ~50 nm in Ca^{2+} exchangeable forms.

Fig. 3 TEM micrographs showing keggin treated smectite display compacted taktoid sheet with highly depressed surface loose material layer to maximum 10 nm.

Fig. 4 TXM stereo-pare micrographs (A) shot with 1 degree difference in angle (Sample 0), reveals spongy irregular network of compact tactoids connecting with each other in chain stairstep aggregates assembling cells up to 1.5 µm in diameter (shown as a white bar in left micrograph). The 3-D computer reconstruction (B) shows large cellular pattern of microstructure with thick elongated walls composed of stairstep-like stacked smectite tactoids.

Fig. 5 TXM stereo-pare micrographs shot with 1 degree difference in angle in Sample 1 (gelled by addition of keggin to smectite suspension) reveal single tactoids connected in edge to face and face to face orientation living voids in between particles up to 200 nm in diameter. White spherical particle near the middle of micrograph is gold nano-particle introduced to sample for better alignment.

Fig. 6 Computer 3-D reconstruction of TXM tomography in Sample 1, shows cellular honeycomb like networking between smectite tactoids (scale bar 1 µm).

Fig. 7 TXM stereo-pare micrographs shot with 1 degree difference in angle in Sample 2 (flocked during addition of smectite to dilute keggin solution). Long worm-like stacked aggregates of smectite tactoids are covered by white colloidal blanket.

Fig. 8 Computer 3-D reconstruction of TXM tomography in Sample 2, shows stacked worm-like aggregates with voids in-between them (scale bar 2 µm).

Fig. 9 The 3-D computer reconstruction of TXM tomography in Sample 1, (A) and Sample 2 (B). In this investigations both samples show significant degree of flocculation with fine cellular structure with large voids and thinner walls in Sample 1 and irregular inter-aggregate voids and thick dense aggregates in Sample 2.

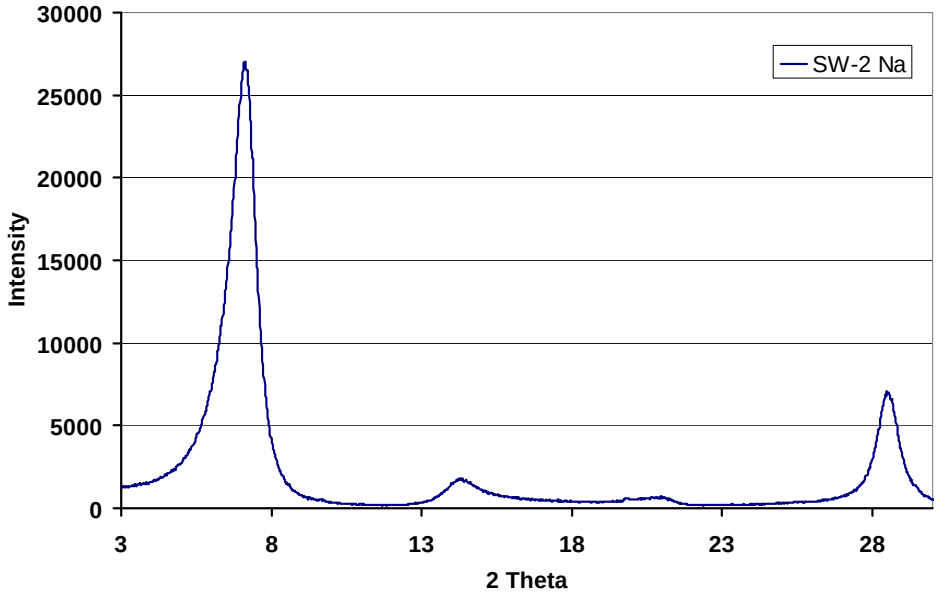
30000
25000
20000
15000
10000
5000
0
Intensity
3
8
13
18
23
28
2 Theta
SW-2 Na

Figure 1a

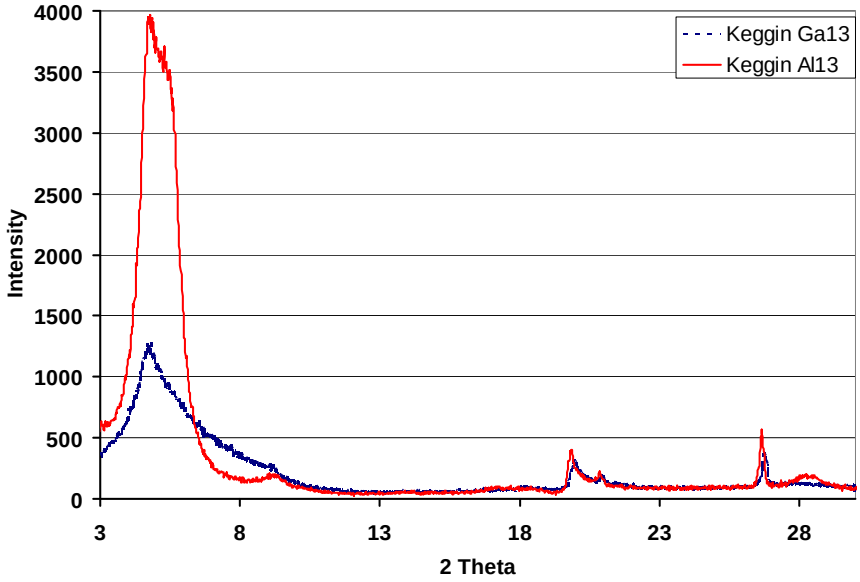
Keggin Ga13
Keggin Al13
Intensity
4000
3500
3000
2500
2000
1500
1000
500
0
3
8
13
18
23
28
2 Theta

Figure 1b

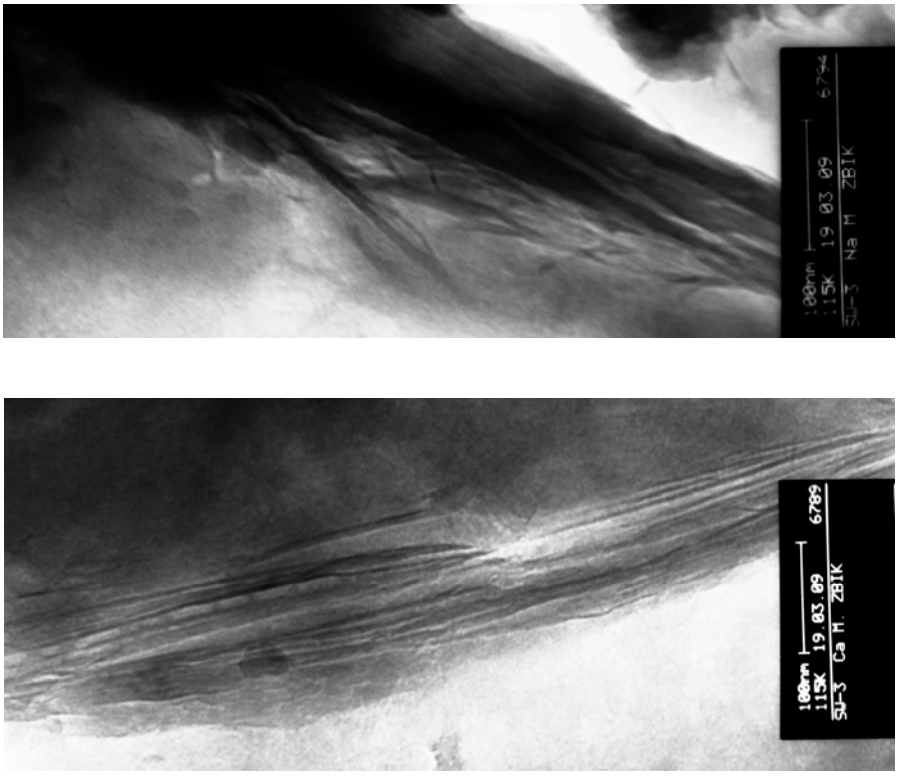
100nm
15K 19.03.09 6794
SU-3 Na M. ZBIK
100nm
115K 19.03.09 6789
SU-3 Ca M. ZBIK

Figure 2

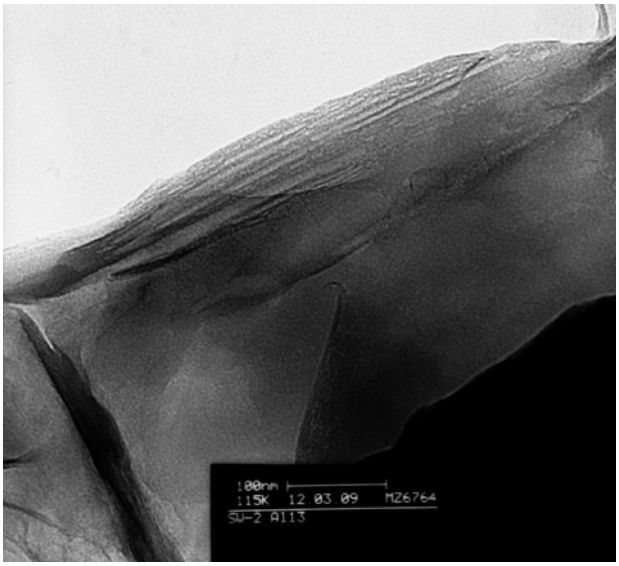
100nm
15K 12 03 09 M26764
SU-2 A113

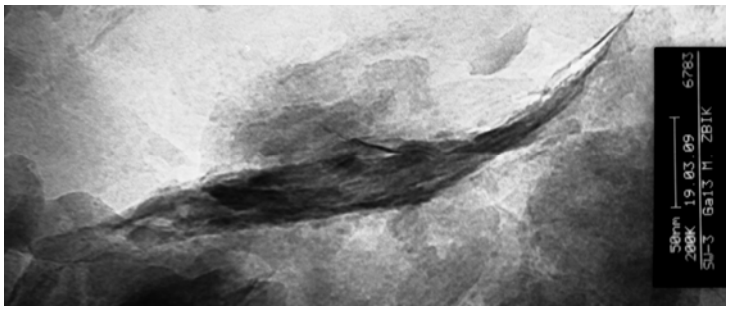
50nm
200K 19 03 09 6783
SU-3 Ga13 M ZB1K

Figure 3

443

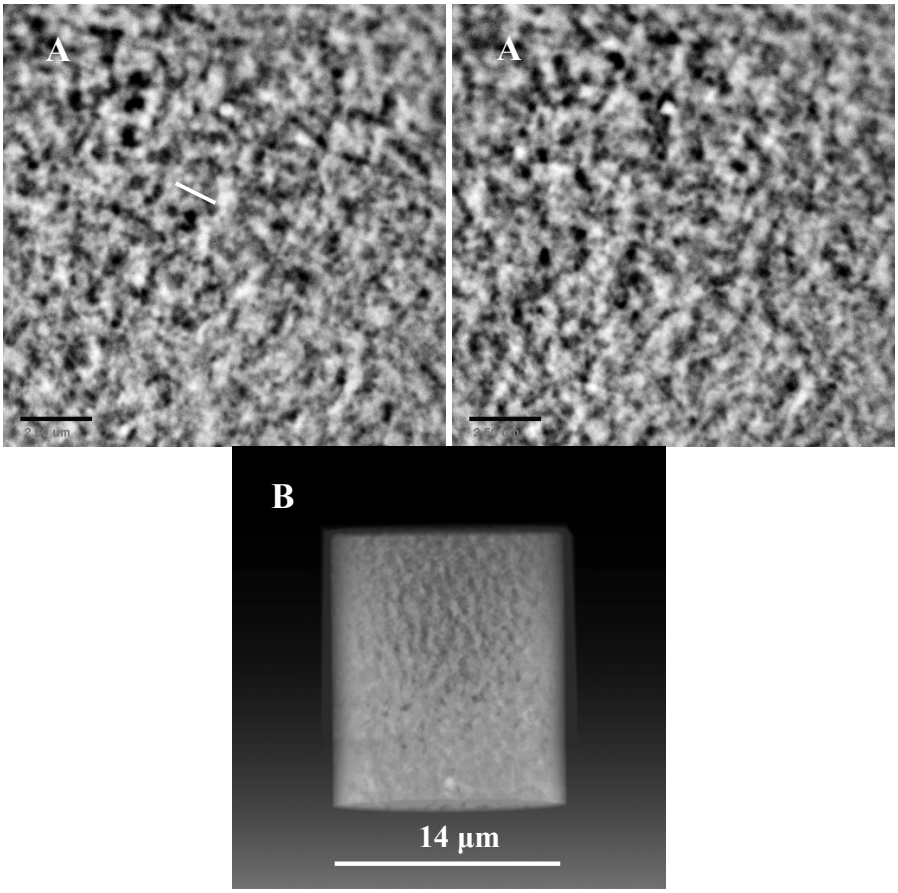

444
445
446

447 **Figure 4**

448
449

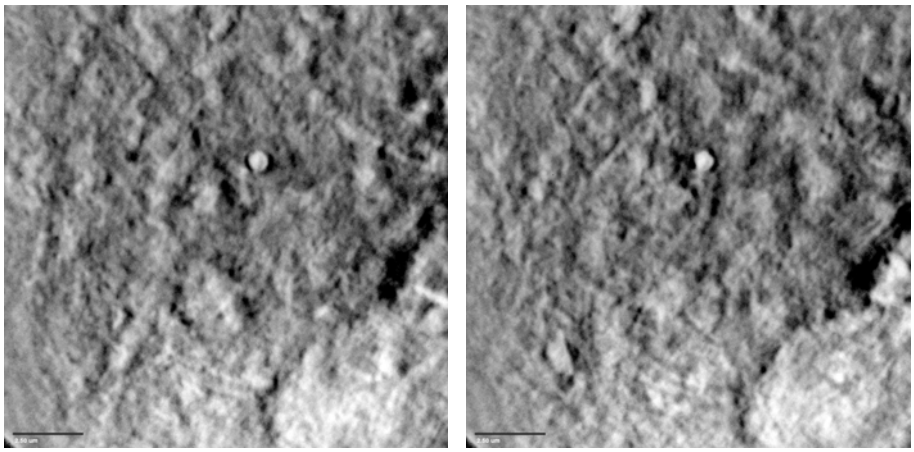

Figure 5

457

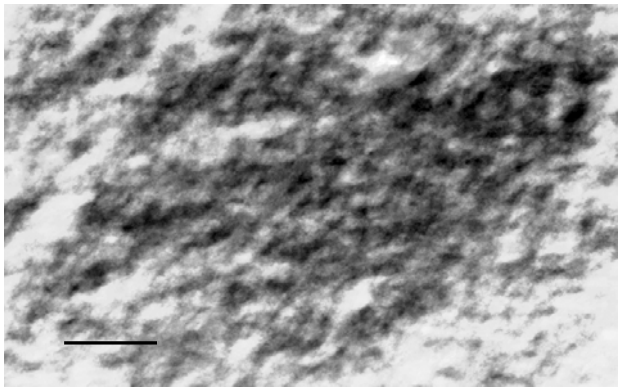

458
459

460 **Figure 6**

461
462

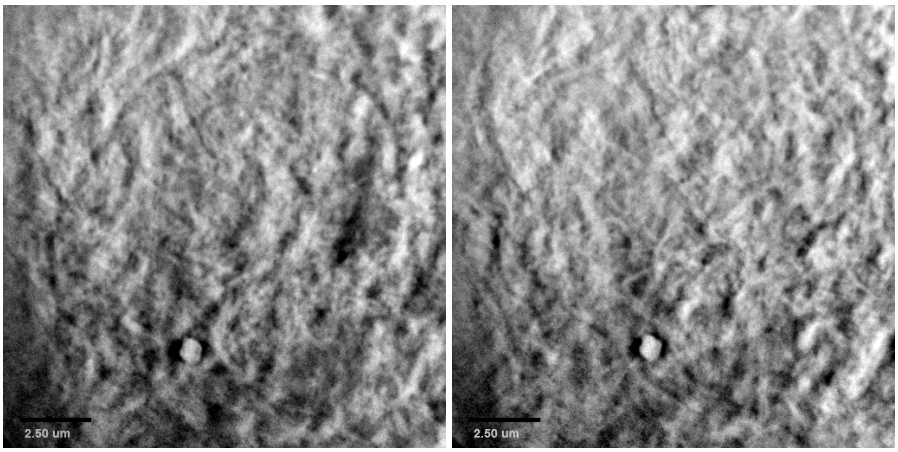

Figure 7

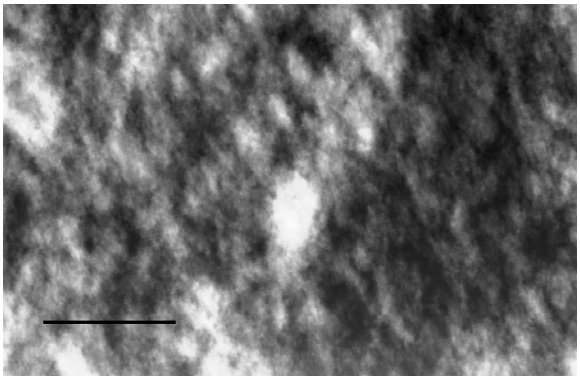

Figure 8

474